ChemComm

FEATURE ARTICLE

View Article Online
View Journal | View Issue

Cite this: *Chem. Commun.*, 2015, **51**, 3024

Hierarchical layered double hydroxide nanocomposites: structure, synthesis and applications

Zi Gu,[a] John James Atherton[ab] and Zhi Ping Xu*[a]

Received 30th September 2014,
Accepted 10th December 2014

DOI: 10.1039/c4cc07715f

www.rsc.org/chemcomm

Layered double hydroxide (LDH)-based nanocomposites, constructed by interacting LDH nanoparticles with other nanomaterials (*e.g.* silica nanoparticles and magnetic nanoparticles) or polymeric molecules (*e.g.* proteins), are an emerging yet active area in healthcare, environmental remediation, energy conversion and storage. Combining advantages of each component in the structure and functions, hierarchical LDH-based nanocomposites have shown great potential in biomedicine, water purification, and energy storage and conversion. This feature article summarises the recent advances in LDH-based nanocomposites, focusing on their synthesis, structure, and application in drug delivery, bio-imaging, water purification, supercapacitors, and catalysis.

1. Introduction

Recent developments in material chemistry and nanotechnology have enabled scientists to develop various nanocomposites by combining different nanomaterials or modifying nanomaterials with functional molecules. The synthesised nanocomposites possess appealing and unique properties that render them attractive for application in healthcare, environmental remediation, and energy storage and conversion.[1–7]

Building tailored layered double hydroxide (LDH)-based nanocomposites is an emerging area in the field of constructing 3-dimensional (3D) hierarchical nanoarchitectures with multiple functionalities. Inorganic LDH compounds, also known as hydrotalcite-like materials or anionic clays, can be found naturally as minerals and can also be readily

[a] *Australian Institute for Bioengineering and Nanotechnology, The University of Queensland, Brisbane, QLD 4072, Australia. E-mail: z.gu@uq.edu.au, gordonxu@uq.edu.au; Fax: +61 07 33463973; Tel: +61 07 33463809*
[b] *Royal Brisbane and Women's Hospital, Brisbane, QLD 4006, Australia. E-mail: john.atherton@health.qld.gov.au; Fax: +61 07 36463257; Tel: +61 07 36460586*

Zi Gu

Dr Zi (Sophia) Gu received her PhD in biomedical engineering from The University of Queensland (with Professor Max Lu) in 2011. She is currently honoured with a National Health and Medical Research Council (NHMRC) Early Career Fellowship at Australian Institute for Bioengineering and Nanotechnology, The University of Queensland. Dr Gu has published more than 10 peer reviewed journal articles (9 first-authored) with over 150 citations in the field of nanobiomaterials. Her current research interests include novel nanostructured materials and their applications in drug/gene delivery and bio-imaging.

John J. Atherton

Dr John Atherton is the Director of Cardiology, Royal Brisbane and Women's Hospital and Associate Professor, The University of Queensland. His research interests include cardiac genetics, heart failure epidemiology and investigating novel methods to detect presymptomatic disease. He sits on the Board of the Cardiac Society of Australia and New Zealand (CSANZ), chairs the CSANZ Professional Ethics Standards Committee, is a member of the National Heart Foundation Heart Failure Guidelines executive writing group, and an appointed member of the Australian Government Medical Services Advisory Committee. He previously chaired the Asia-Pacific Acute Decompensated Heart Failure Registry SAC and the CSANZ Heart Failure Council.

synthesised in the laboratory.[8] They consist of hydroxide layers of different metal cations and interlayer spacing occupied by anions and water molecules.[8] At present, LDH nanoparticles can be tailored with the hydrodynamic diameter from 30–40 nm to 5–10 μm using various hydrothermal treatment methods.[9–11] In addition, through various delamination or top down methods, single-layer LDH nanosheets can be prepared, with the lateral size from 20 nm to several micrometres.[12]

Due to their rich ionic surface –OH group and the inherent positive charge, LDH nanoparticles or nanosheets can interact with other nanomaterials or polymeric molecules, generating 3D nanocomposites with particular architectures. We classify LDH-based nanocomposites into four groups, *e.g.* core@LDH, LDH@shell, dot-coated LDH, and targeting moiety functionalised LDH (Fig. 1). In the core–shell structure, the tailorability and functionality of LDH endow LDH with a dual role. LDH can be the shell component that is used to modify other nanoparticles including silica nanoparticles, magnesium ferrite nanoparticles, *etc.* (Fig. 1A), and can also be fabricated as the core coated by other nanomaterials, such as the silica shell or the polymeric molecule shell (Fig. 1B). The dot-coated LDH is a new group of composites with smaller silica or metal nanoparticles being deposited on the surface of LDH (Fig. 1C). Conjugating antibodies, other biopolymers or folic acid on LDH provides an opportunity for LDH targeting to the site of disease (Fig. 1D).

With the rapid progress of nanocomposite fabrication, the research focus has been gradually shifted to practical applications with the potential of influencing our daily living conditions. The synthesised nanocomposites often possess the merits and functions of individual components, thus showing advantages over the sole nanomaterial.[13] There are fewer published applications on environment and energy; nevertheless, the nanocomposites including silica@LDH,[14,15] metal oxide@LDH,[16] LDH@metal,[17,18] LDH@polymer,[19] folic acid–conjugated LDH,[20] *etc.*, have shown promise as drug delivery vectors, water pollutant removers, high-capacity supercapacitors, and cost-effective catalysts.

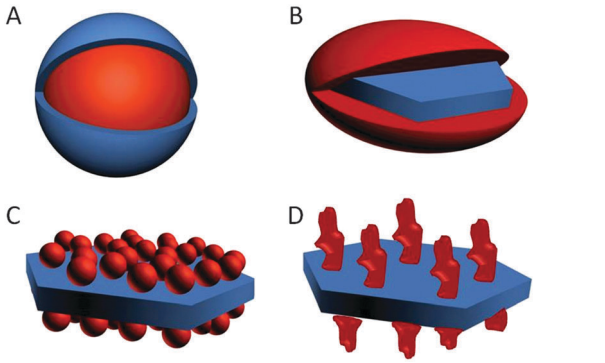

Fig. 1 Schematic illustration of LDH-based nanocomposites with different structures: (A) core@LDH (blue: LDH, red: SiO_2 nanoparticles, or magnesium ferrite nanoparticles, *etc.*), (B) LDH@shell (blue: LDH, red: SiO_2 nanoparticles, protein, polymer, organic hydrophobic modifier, *etc.*), (C) dot-coated LDH (blue: LDH, red: metal nanoparticles, SiO_2 nanoparticles, *etc.*), and (D) targeting moiety functionalised LDH (blue: LDH, red: folic acid, antibody, *etc.*).

Tailoring the functions of LDH-related nanocomposites is a relatively new area, yet rapidly evolving area, with a significant increase in the number of publications over the last 10 years (approximately 10-fold annual increase from 2004 to 2013; source from Web of Science). In 2013, Duan and co-workers published a review focusing on the magnetic nanoparticle@LDH core–shell nanostructure. Until now no review paper has comprehensively summarised the basic strategies to construct 3D hierarchical LDH-based nanocomposites and their applications in the fields of biomedicine, environment remediation, and energy conversion and storage. Thus we believe that it is timely to review the latest research progress on hierarchical LDH-based nanocomposites. In this feature article, we summarise the recent advances in design, fabrication and potential applications of LDH-based nanocomposites with a highlight on biomedical applications, and our focus is to link a particular potential application to the hierarchical structure and building components of the corresponding nanocomposites. After a brief review of LDH nanoparticles and nanosheets in terms of concept, synthesis and applications (Section 2), the LDH-based core–shell nanoparticles are reviewed as core@LDH (Section 3) and LDH@shell (Section 4), respectively. The dot-coated LDH nanocomposites and targeting moiety-conjugated LDH nanocomposites for targeted delivery are reviewed in Sections 5 and 6, respectively. In each section, we examine closely the synthesis approaches, structures, and key potential applications. In the final section (Section 7), we provide our perspectives on the future developments in fabrication and application of LDH-based nanocomposites.

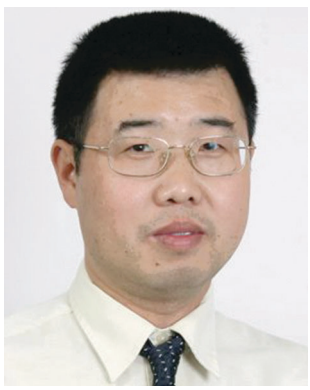

Zhi Ping Xu

Dr Zhi Ping Xu obtained his BS degree from the University of Science and Technology of China (Hefei, China) in 1988, and received his PhD degree from National University of Singapore in 2001. After his postdoctoral fellowship at University of North Texas, he joined the Australian Institute for Bioengineering and Nanotechnology, the University of Queensland as a research fellow in 2004, and an associate professor since 2011. He has published over 160 journal papers, and his current research focuses on developing clay and clay-hybrid nanomaterials for drug/gene/vaccine delivery to treat tumour and infectious diseases, as well as for chemical catalysis.

2. LDH nanoparticles and nanosheets

LDHs consist of brucite-like layers containing hydroxides of metal divalent and trivalent cations (M^{2+} and M^{3+}, such as Mg^{2+}, Zn^{2+},

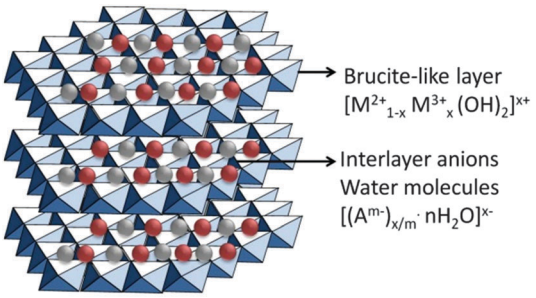

Fig. 2 Schematic illustration of layered double hydroxide structure and chemical components.

Ni^{2+}, Al^{3+}, and Fe^{3+}). Each cation is octahedrally surrounded by six OH^- ions, and the different octahedra share edges to form a 2D layer. Between the brucite-like layers there are exchangeable anions (A^{m-}, such as CO_3^{2-}, Cl^-, and NO_3^-). The substitution of M^{2+} by M^{3+} in the hydroxide layer results in a positive charge, which is neutralised by the interlayer anion (A^{m-}). The interlayer space also contains water molecules, hydrogen bonded to layer OH^- and/or to the interlayer anions. Due to the electrostatic interactions and hydrogen bonds, the LDH forms the layered structure (Fig. 2). The general formula for these LDHs can be written as $[M^{2+}_{1-x}M^{3+}_{x}(OH)_2]^{x+}(A^{m-})_{x/m}\cdot nH_2O$, where x = 0.2–0.33, which means the M^{2+}/M^{3+} molar ratio is 2.0–4.0.[8,12,21] The layer may also consist of monovalent and quadrivalent cations such as Li^+ and Ti^{4+}.[8]

Various facile synthesis methods have been studied and used to prepare LDH nanoparticles. Co-precipitation and anion exchange are the most common ones in the laboratory and conducted by simultaneously precipitating metal cations at constant or varied pH. The comprehensive study of LDH physicochemical properties and synthesis methods has led to wide applications including drug delivery carriers,[22] biosensors,[23] water treatment agents,[24] catalysts,[25] supercapacitors,[26] *etc.* Due to the interlayer anions in the LDH gallery being exchangeable, various negatively charged therapeutic molecules and pollutants in wastewaters can be intercalated into the interlayer and adsorbed on the LDH surface, which could allow effective therapy and wastewater treatment, respectively.[27–29] LDHs containing transition-metal elements are used as supercapacitor electrode materials, because the layered structure of LDHs provides a homogeneous dispersion of transition-metals in the matrix.[30]

In recent years, LDH nanosheets are attracting great attention. Thanks to their 2D anisotropy with around one nanometer in thickness and tens to thousands of nanometres in lateral dimension, LDH nanosheets contribute tremendously to fundamental research and their application in building functional nanocomposites.[12] In general, LDH single sheets can be synthesised by two approaches, *i.e.* delamination of LDH nanoparticles and one-step synthesis of LDH monolayers.[12] Delamination of LDH nanoparticles can be achieved by using a wide variety of solvents, including butanol, acrylates, formamide, *etc.*;[31–33] and the one-step synthesis method employs a reverse microemulsion approach.[34,35] The charged nanosheets can be assembled to produce various nanoconjugates, nanofilms, and nanoarchitectures, which have tremendous potential applications in biomedicine, energy storage and energy conversion.[36–38]

3. Core@LDH nanocomposites

The core@LDH nanocomposites are equipped not only with the unique physicochemical properties (*e.g.* nanometre size and layered structure), but also with new and interesting functions (*e.g.* magnetism, porous structure, and high surface-to-volume ratio). We will summarise the synthesis strategy and morphology of the core@LDH nanocomposites, and their applications in drug delivery, water purification, and energy conversion and storage in this section.

3.1 Synthesis of the LDH shell

The method of LDH shell synthesis is generally grouped into three categories: (1) coprecipitation; (2) the sol–gel method; and (3) direct deposition (Fig. 3). Coprecipitation is a traditional and most commonly used method in the laboratory. The sol–gel method is a new and interesting approach where AlOOH primer sol serves as the substrate as well as the aluminium source. Different from the coprecipitation and the sol–gel method in which LDH grows *in situ* on the core, direct deposition is conducted by grafting pre-synthesised LDHs on the core surface, and especially useful to fabricate the shell consisting of LDH nanosheets.

3.1.1 Coprecipitation. Coprecipitation is a facile and commonly used method for synthesising the LDH shell. The cores that have been widely studied include silica nanospheres, metal oxide nanoparticles and nanowires, and the shells produced by coprecipitation are always LDH nanoparticles. In general, the core adsorbs two different metal cations that are subsequently precipitated on the surface of the core, and the LDH crystal growth occurs by aging at a certain temperature or through hydrothermal treatment (Fig. 3A). Zhang *et al.* used the coprecipitation method to prepare an anti-inflammatory drug-loaded LDH shell on the magnesium ferrite core.[14,39] In this work,

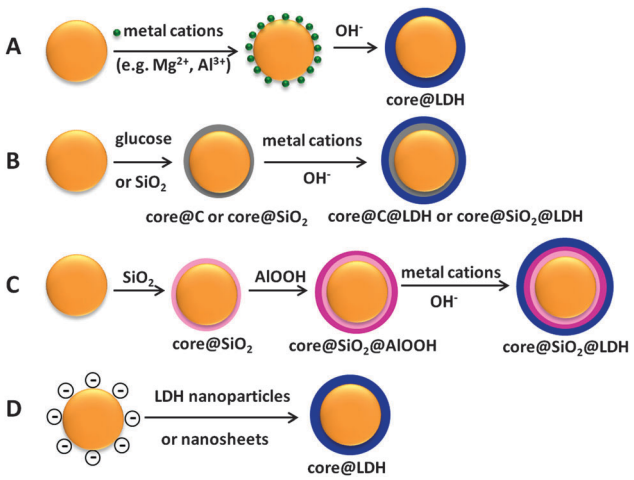

Fig. 3 Schematic illustration of the fabrication of core@LDH nanocomposites by coprecipitation (A, B), sol–gel (C), and direct deposition (D).

the magnesium ferrite particle core that first adsorbed Mg^{2+} and Al^{3+} cations was mixed with a solution containing sodium hydroxide and diclofenac or ibuprofen to precipitate.[14,39] The synthesised magnetic drug–LDH nanohybrid possessed a clear core–shell structure with a diameter around 100 nm.[14,39] An earlier study by Zhang *et al.* reported a similar core–shell nanostructure by using the coprecipitation method.[40] However, they failed to produce homogeneous core–shell structured particles, and the particles had a network-like morphology where particle aggregation occurred. Following careful examination of the experiments in these two papers, we reasoned that ultrasonication might be a critical factor, facilitating metal cations to be evenly distributed and adsorbed on the surface of the core material and thus improving homogeneous growth of LDH. The ultrasound-assisted coprecipitation method has also been applied to synthesise a variety of core@LDH nanocomposites, such as SiO_2@LDH,[15] Fe_3O_4@LDH,[16] and Y_2O_3:Er^{3+},Yb^{3+}@SiO_2@LDH.[41]

In order to fabricate the homogenous LDH nanostructure on the surface of a ferrite core, pre-coating the core by a thin layer of carbon (C–OH) or silica (SiO_2) prior to coprecipitation has been examined (Fig. 3B). A thin layer of carbon coating by the polymerisation and carbonisation of glucose through a hydrothermal reaction generates large amounts of hydrophilic groups C–OH, which facilitates the formation of the LDH shell on the ferrite core.[42] Silica, due to its surface active –OH group, can interact effectively with metal oxide nanospheres or LDH nanoparticles to form metal oxide@SiO_2@LDH nanocomposites.[36] Taking advantage of this unique property of silica, Chen *et al.* coated Y_2O_3:Er^{3+},Yb^{3+} nanophosphors with a layer of silica and then precipitated metal cations to form LDH nanoparticles on the surface of the silica layer, and thus generated a Y_2O_3:Er^{3+},Yb^{3+}@SiO_2@LDH core–shell nanoarchitecture.[41]

3.1.2 Sol–gel method. The first sol–gel method to fabricate LDH shells was reported by Wei and co-workers in 2010.[43] In this method, the boehmite (AlOOH) primer sol prepared by hydrolysing the precursor $Al(OPr)_3$ was deposited on the scaffold (*i.e.* paper, cloth or sponge) with several cycles of sol–gel deposition (Fig. 3C).[43] The generated AlOOH coating as both substrate and source of aluminium resulted in LDH *in situ* growth on the scaffold (Fig. 3C).[43] Using this method, Shao *et al.* successfully synthesised SiO_2@LDH and Fe_3O_4@SiO_2@LDH core–shell composites with diameters of ~600 nm and ~900 nm, respectively.[44,45] Based on the SiO_2@LDH core–shell structure and the sol–gel method, the same group also synthesised a SiO_2@LDH yolk–shell and hollow structure by adjusting the concentration of urea.[44] Using the sol–gel method, Wang *et al.* coated a much smaller SiO_2 core (50 nm, compared with Wei *et al.*'s 340 nm) with LDH and generated SiO_2@LDH core–shell nanocomposites.[46] The sol–gel method can also be applied to grow LDH on the carbon-coated Fe_3O_4, but failed to produce well-dispersed, homogenous core–shell particles.[47]

3.1.3 Direct deposition. In the direct deposition approach, the core material and LDH nanoparticles or nanosheets are synthesised separately, and subsequent combination of these building blocks generates a core–shell structure by self-assembling, followed by some post-treatment (Fig. 3D). Ay *et al.* and Li *et al.* used the direct deposition method to synthesise magnetic metal oxide core@LDH shell nanocomposites by adsorbing LDH nanoparticles on the core surface.[48,49] Li *et al.* also investigated the effect of post-aging temperature on the structure and physicochemical properties of the core–shell nanocomposites. With the temperature increasing from 100 to 160 °C, the LDH particles increased in size and crystallinity, and the morphology of LDH changed from flocculent-like to platelet-like shape.[49] Very interestingly, Choy and co-workers formulated bio core@inorganic shell nanohybrids with a size of around 100 nm by mixing designed DNA solution (negatively charged) and a solution containing LDH nanosheets (positively charged) together.[50] The transmission electron microscopy image of this nanocomposite showed a clear core (biomolecule, *e.g.* DNA)–shell (LDH) structure with the shell of ~10 nm thickness. Nonetheless, accurate control of deposited LDH density remains a challenge.

Coating LDH nanosheets on the core sphere *via* layer-by-layer deposition produces a multi-layered LDH shell in a controlled manner. Sasaki's group fabricated a polystyrene bead@LDH nanosheet core–shell microsphere by depositing 20 layers of poly(sodium 4-styrene sulfonate)–LDH nanosheets.[51,52] The core was later on used as a sacrificial template in this work. Based on this technique, Li *et al.* synthesised functional Fe_3O_4–SiO_2 core coated with 20 layers of alternating carbonate and LDH nanosheets ($(CO_3^{2-}/LDH)_{20}$).[53]

Electrodeposition is a widely applied coating technique in industry to graft one material on the other, and this is also useful to assemble LDH nanoparticles or nanosheets on nanowires.[54] Using this method, LDHs with positive charges are suspended in water and migrate towards the electrode scaffold (*i.e.* nanowire) under the influence of electrophoresis to construct a 3D hierarchical metal oxide nanowire@LDH nanoarchitecture.[54]

3.2 Morphology of core@LDH nanoparticles

In general, the LDH shell in the core–shell nanoarchitectures possesses three different but interactive morphologies, *i.e.* horizontally oriented platelets, vertically oriented platelets, and mixed platelets (Fig. 4). The horizontally oriented platelet morphology tends to be formed by direct deposition of LDH nanosheets on the core materials (described in Section 3.1.3) and possibly by coprecipitation (described in Section 3.1.1).[50,53] The LDH nanosheets have a high aspect ratio, large surface area, and desirable flexibility to be curved, which facilitate the nanosheets to adhere horizontally onto the sphere core. The vertically oriented platelet morphology is an interesting one that creates a porous structure, thus favoured by the researchers in the area of drug delivery and water purification. The LDH shell oriented vertically on the core is often generated by the sol–gel method (described in Section 3.1.2) and sometimes by coprecipitation.[41,44,45,55] The coexistence of horizontally and vertically oriented platelets leads to the formation of the third morphology, *i.e.* mixed platelets. The mixed platelet morphology was firstly denoted by Zhang *et al.* who fabricated magnetic

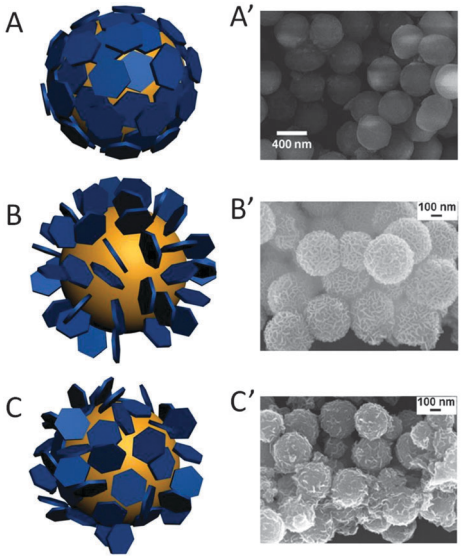

Fig. 4 Schematic illustration and SEM images of core@LDH nanoarchitectures with different morphologies: horizontally oriented platelets (A, A′), vertically oriented platelets (B, B′), and mixed platelets (C, C′). Images A′–C′ are reproduced from ref. 53 and 55 with permission.

core@LDH shell nanocomposites using the coprecipitation method.[14] This type of morphology has been seen in most cases of coprecipitation and direct deposition,[42,55] and sometimes in the sol–gel method.[46]

The linkage between the LDH shell and the metal oxide core has been proposed as MI–O–MII bonds where MI and MII represent metal cations from LDH and the core, respectively.[40,56] There are two possible interactions between the core and the shell *via* MI–O–MII bonds: (1) MI–O–MII bonds perpendicular to the LDH layer generate the horizontally oriented LDH shell, and (2) MI–O–MII bonds parallel to the LDH layer form the vertically oriented LDH shell.[40] Zhang *et al.* suggested that the vertically oriented LDH morphology is more easily formed because of the more unsaturated sites localised near the edge of LDH layers.[40] However, they did not give explanation for the formation of the horizontally oriented LDH shell. More recently, Chen *et al.* synthesised Fe_3O_4@LDH core–shell nanocomposites with different morphologies by adjusting the methanol/water solvent ratio.[55] They found that the vertically orientated morphology was formed in the water (no methanol) environment, and the mixed morphology formed in the solvent containing methanol and water (volume ratio 1 : 1).[55] In their proposed mechanism, the formation of the former structure, *i.e.* the vertically oriented LDH, is due to the rapid nucleation of LDH compactly packed on the core surface, simultaneously upon the LDH crystal growth on the (110) plane faster than on the (003) plane.[55] Unfortunately, they did not illustrate the formation mechanism of the mixed morphology.

Here, we tentatively propose an assumption to explain the mechanism of different LDH shell morphologies formed by coprecipitation based on the formation mechanism of the vertically oriented LDH on Fe_3O_4 nanoparticle cores proposed by Chen *et al.*[55] When nucleation is fast, *e.g.* high supersaturation,

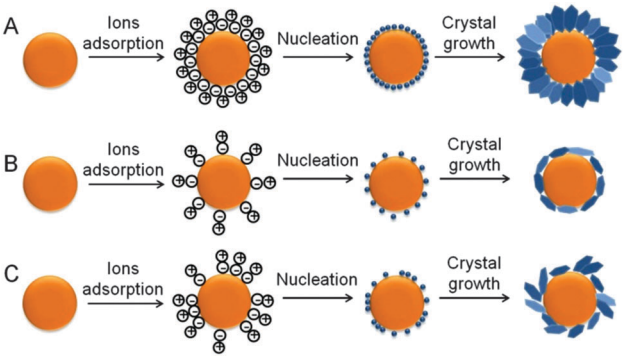

Fig. 5 Schematic illustration of formation of core@LDH nanocomposites with (A) vertically oriented, (B) horizontally oriented, and (C) mixed platelet morphology.

the LDH nuclei are compactly packed on the core surface. Because of the limited growth space, the horizontally oriented nuclei initially formed are sacrificed and subsequently contribute to the crystal growth of the vertically oriented LDHs. Eventually, the vertically oriented LDH shell morphology becomes dominant with the growth along (110) more readily accessible than that along (003) (Fig. 5A). On the other hand, when the nucleation rate is severely restricted by some factors such as the low supersaturation or solvent, the LDH nuclei are sparsely attached on the core. As the LDH nuclei grow, the relatively smaller vertically oriented LDHs (due to the restriction of growth by the core) are sacrificed, and thus the relatively larger horizontally oriented LDH crystals become dominant (Fig. 5B). In the situation between these two cases, the mixed platelet morphology forms (Fig. 5C). To the best of our knowledge, no one reports the horizontally oriented morphology of the LDH shell formed by coprecipitation, while we still suggest the possibility to tailor the morphology of the nanocomposites by properly controlling the nucleation rate based on our assumption. Therefore, synthesis conditions that influence the nucleation rate need to be carefully examined in order to design and fabricate LDH-coated nanocomposites with a specific morphology.

3.3 Applications of core@LDH nanocomposites

Owing to their unique properties such as high surface area, magnetism and porous structure, the core@LDH nanocomposites have been examined for their application in drug delivery, water purification, and energy conversion and storage.

3.3.1 Drug delivery. Drug delivery, as one of the most important applications of functional core@LDH nanocomposites, allows ideally sustained, controlled, and/or targeted delivery of therapeutic compounds with the aim of improving their therapeutic effects. The core provides a matrix for the shell growth, and more importantly endows the nanocomposite with extra functional properties, such as ferric magnetism and superparamagnetism. The LDH shell serves as an efficient drug host by intercalating/releasing the drug/gene anions into/from the LDH interlayer,[27,57,58] as the interlayer anions of LDHs can be exchanged with other anions in the medium with the affinity order of $CO_3^{2-} > HPO_4^- > CrO_4^- > SO_4^{2-} > OH^- > F^- > Cl^- > Br^- > NO_3^- > I^-$.[8] Drug/gene anions are released from

the LDH shell by diffusing from the LDH interlayer and/or by LDH layer dissolution, and the drug/gene release from the composites always shows a sustained release profile, in which an initial burst release can quickly establish the therapeutic dose and the subsequent prolonged release maintains this dose for a long period of time.

The drugs intercalated in the LDH shell include anti-inflammatory drugs (*e.g.* diclofenac, ibuprofen, and glucuronic acid),[14,56,58] anti-cancer drugs (*e.g.* doxorubicin, doxifluridine, and 5-fluorouracil),[41,42,49] and hepatitis B virus DNA vaccine.[46] Wang *et al.* synthesised SiO_2@LDH nanocomposites with an average diameter of 210 nm and mixed platelet morphology.[46] They claimed that the most important advantage of this nanocomposite over other nanomaterials was its larger surface area, which could allow the loading and delivery of a large amount of DNA vaccine.[46] They also found that DNA vaccine loaded-SiO_2@LDH immunised mice demonstrated much higher serum antibody response than naked DNA vaccine, and enhanced T-cell proliferation and skewed T helper to Th1 polarisation.[46] In the physiological environment, the loaded drugs are released in a sustained manner from the nanocomposites by anion exchange and/or nanocomposite biodegradation.[27]

Zhang *et al.* designed a controlled drug release device by coprecipitating the mixed platelet LDH shell with diclofenac loading on the magnesium ferrite nanoparticle core (Fig. 6A).[14] Under an external magnetic field, they observed a decreased drug release rate (~20% decrease) in pH 7.45 phosphate buffer saline (PBS), which is presumably resulted from the aggregation of the magnetic nanocomposites triggered by magnetic force (Fig. 6B and C).[14,39] This group also claimed that the overall release profile was determined by three diffusion paths of the loaded drug from the magnetic nanohybrids (Fig. 6D): (I) intra-particle diffusion from the LDH interlayer space to the LDH interparticle space, (II) interparticle diffusion from the space among the LDH particles to the inter-aggregate space, and (III) inter-aggregate diffusion from the space among the core–shell particle aggregation to solution.[14] When the magnetic field was applied, the magnetic core–shell nanohybrids aggregated, leading to longer diffusion length, higher diffusion resistance, and a decreased drug release rate (Path III) (Fig. 6B and D).[14,39] Apart from the controlled release, targeted delivery of drugs to the diseased site using the magnetic core–shell nanohybrids is also promising with the application of an external magnetic field.[58] The magnetic drug delivery system concentrates the drug dosage at a target site with the aid of an external magnetic field, thus avoids nonspecific drug delivery, enhances the therapeutic effect and reduces the drug side effects.[59,60] The targeted delivery can also be achieved by conjugating antibody and other ligands on the LDH nanoparticles,[49,61] and will be described in detail in Section 6.

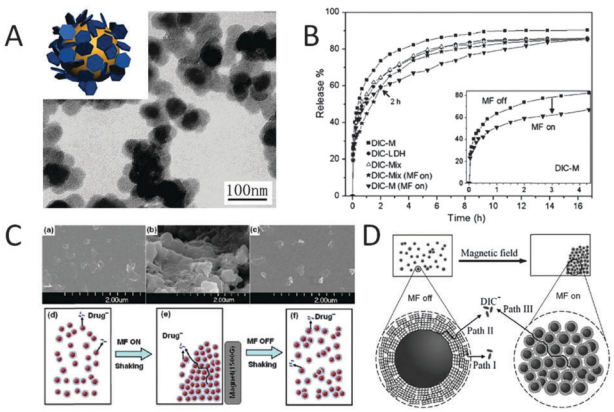

Fig. 6 (A) TEM image of diclofenac-loaded magnesium ferrite nanohybrids (DIC-M) with the mixed platelet LDH shell. The inset shows the schematic illustration of DIC-M core@shell morphology with the mixed platelet shell. (B) Release curves of DIC from DIC-M, DIC-LDH and the DIC-loaded physical mixture of magnetic nanoparticles and LDH (DIC-Mix) in pH 7.45 PBS. The inset shows the release curves of DIC-M with and without an external magnetic field. (C) SEM images and schematic illustration of the magnetic nanoparticle@LDH nanohybrid: (a, d) without an external magnetic field, (b, e) with an external magnetic field, and (c, f) when removing the magnetic field. (D) Three diffusion paths of the loaded drugs from the magnetic nanoparticle@LDH nanohybrid: (I) intraparticle diffusion from the LDH gallery space, (II) interparticle diffusion from the space among the LDH particles, and (III) interparticle diffusion from the space among particle aggregates to solution. Modified and reproduced from ref. 14 and 39 with permission.

3.3.2 Water purification. Pollutants in waste waters or aquatic systems have become an emerging environmental and health issue.[62,63] In recent years, adsorption by LDH-consisted core–shell nanoarchitecture *via* ion exchange is recognised as an efficient and low-cost approach to remove pollutants (*i.e.* acidic pharmaceutical compounds, fluoride, and heavy metal) from waste waters.[15,16,47]

Chen *et al.* reported a typical vertically oriented SiO_2@LDH core–shell nanocomposite synthesised by ultrasound-assisted coprecipitation (Fig. 7A), which showed much more efficient

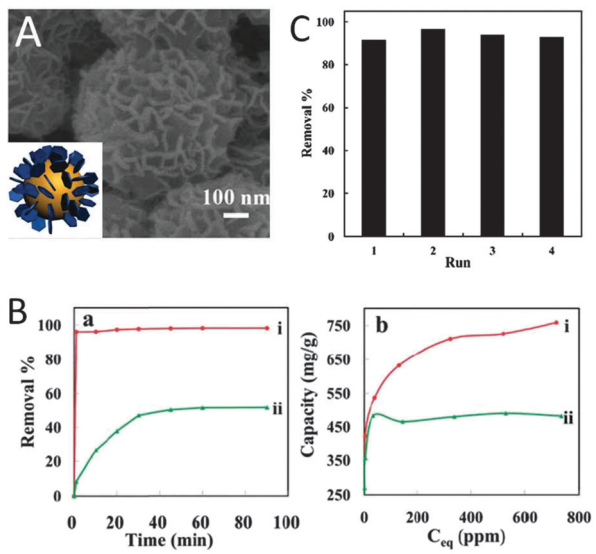

Fig. 7 (A) SEM images of SiO_2@LDH nanocomposites. The inset shows the schematic illustration of their vertically oriented platelet core–shell morphology. (B) Kinetic study (a) and the adsorption isotherm (b) of diclofenac on (i) SiO_2@LDH and (ii) LDH. (C) Percentage of diclofenac removal using SiO_2@LDH in cycle runs. Modified and reproduced from ref. 15 with permission from The Royal Society of Chemistry.

adsorption of diclofenac (a typical pharmaceutical pollutant) than LDH aggregates in terms of the adsorption rate and capacity (Fig. 7B).[15] They found that the higher adsorption capacity of diclofenac on this core–shell nanocomposite (758 mg g^{-1}) than that on LDH aggregates (489 mg g^{-1}) was mainly related to the large surface area of the vertically oriented LDH shell (Fig. 7B).[15,64] The adsorption capacity of diclofenac by SiO_2@LDH (758 mg g^{-1}) is also obviously higher than that by polymers (324.8 mg g^{-1})[64] and mesoporous silica (0.34 mg g^{-1}).[65] The magnetic nanoparticle@LDH core–shell nanocomposites have also been synthesised to remove fluoride ions and uranium(VI) from aqueous solutions.[16,47]

After pollutant adsorption, regeneration and re-utilisation of the spent adsorbents is a vital process in large-scale cost-effective wastewater treatment. The feasible and efficient approaches to regenerating core@LDH nanohybrid adsorbents include (1) advanced oxidation to decompose the adsorbed compounds and (2) desorption of the pollutant in the eluent to re-use.[15,16,47,66] With advanced oxidation, Chen *et al.* reported the removal efficiency of SiO_2@LDH being consistently above 90% for at least four runs by using Co^{2+} ions and ozone as the catalyst and oxidant, respectively (Fig. 7C).[15] The desorption efficiency is dependent on the affinity of intercalated anions in the LDH-based adsorbent and the anions in the eluent. In general, the eluent containing CO_3^{2-} had the highest desorption efficiency of around 80%.[16,47]

3.3.3 Energy conversion and storage. Many efforts have been made to develop efficient and sustainable energy storage and conversion approaches because of ever worsening energy depletion and global warming.[67–69] The core@LDH nanocomposites with enhanced supercapacitor and catalyst behaviour can be potentially applied in energy storage and conversion devices.[56]

The characteristic properties of a supercapacitor candidate include high redox activity, high surface area, and suitable mesopore/micropore size distribution. Researchers have found that the synthesised 3D hierarchical core@LDH architectures possess these properties, and show excellent supercapacitive performance in terms of capacitance, energy density, and the cycling rate.[44,54,70] With different synthesis methods applied (such as deposition and sol–gel), these core@LDH architectures always have vertically orientated or mixed platelet morphology which allows the nanocomposite to form porous structure and enlarge the surface area to the maximum extent.[44,54,70] The different interior hierarchy structures (SiO_2@LDH core–shell, yolk–shell, and hollow LDH shell) have also been compared in their supercapacitive performance. Shao *et al.* showed that the hollow NiAl–LDH structure had greatly improved faradaic redox reaction and mass transfer, and exhibited excellent pseudocapacitance performance because of the large surface area of the hollow structure, which provides effective diffusion channels for the electrolyte ions.[44] Wang *et al.* synthesised a hierarchical NiAl–LDH@mutiwalled carbon nanotube nanocomposite that grew on nickel foam with an exceptional areal capacitance (7.5 F cm^{-2}) and specific capacitance (1293 F g^{-1}).[71] These values are among the highest that are reported so far for other oxide/hydroxide derived architectures, such as NiTi–LDH/NF film (10.37 F cm^{-2}),[72] β-$Ni(OH)_2$/NF (2675 F g^{-1}),[73] hierarchical $Ni_{0.25}Co_{0.75}(OH)_2$ (928.4 F g^{-1} or 9.59 F cm^{-2}),[74] hybrid nickel hydroxide/carbon nanotube (16 F cm^{-2}),[75] and 3D nanostructure CoO@$Ni(OH)_2$ (11.49 F cm^{-2}).[76] This new hierarchical structure shows as a highly promising electrode that can be applied in electrochemical energy storage.[71]

In addition to supercapacitors, core@LDH has been studied as a catalyst to convert acetone to diacetone alcohol as an alternative fuel component at the thermodynamic equilibrium with the conversion of 23% at 273 K.[56] The authors claimed that the catalyst was easily recovered attributed to the magnetic core and reactivity in the second run remained unchanged.[56]

3.3.4 Other applications. Other applications of the core@LDH nanocomposites include immunosensors,[61] a DNA-based document ID system,[50] and purification of recombinant proteins.[45] Fewer studies in these interesting areas may imply that more efforts should be directed into these applications.

4. LDH@shell nanocomposites

Continuous efforts have been dedicated to producing the shell of different matters on the LDH core for application in healthcare, energy conversion and storage. The functionalisation methods, including adsorption, polymerisation, *etc.*, take advantages of LDH surface –OH groups and its surface positive charge. Thanks to the successful innovation of these methods, a variety of functional nanomaterials (*i.e.* silica nanoparticles, polymers, and proteins) and small molecules (*i.e.* surfactant and folic acid) have been anchored on the LDH core to form various LDH@shell nanocomposites. This kind of combination can be regarded as the surface modification of LDH nanoparticles to improve LDHs' functionality, and also viewed as combining the advantages and functions of the LDHs and the functional nanomaterials for their practical applications, such as drug delivery, imaging, catalysis, and energy storage, as summarised in this section.

4.1 LDH@SiO_2

To encapsulate LDH with SiO_2 to form LDH@SiO_2 nanorattles, tetraethyl orthosilicate $Si(OC_2H_5)_4$ (TEOS) is used as the source of silica, and hydrolysed on the surface of the LDH core (as a nuclear). The linkage between these two inorganic nanomaterials (LDH and SiO_2) is suggested to be –M–O–Si– (M is the metal cation in the brucite-like layer of LDH), as illustrated in Fig. 8.

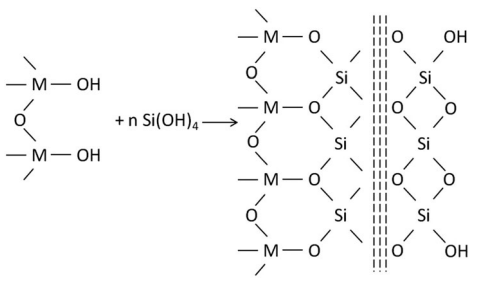

Fig. 8 Schematic illustration of the interaction between LDH and SiO_2 in the LDH@SiO_2 nanostructure. M represents metal cations (*e.g.* Mg^{2+}, Al^{3+}).

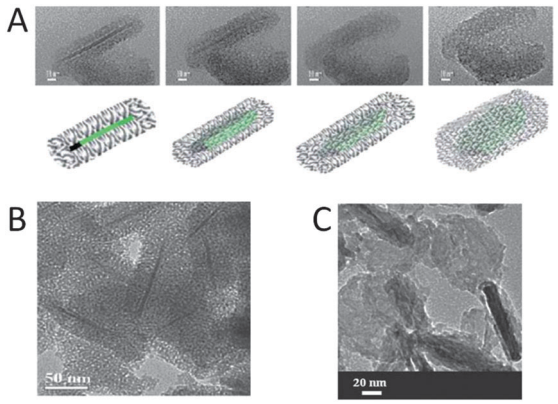

Fig. 9 TEM images of LDH@SiO_2 nanocomposites. The upper images of (A) show the TEM images of one LDH@SiO_2 nanocomposite observed at different angles by tilting the specimen with a step of 10 degree and the bottom pictures of (A) are the corresponding cartoon profile, where the typical nano-rods and nanoplates are shown in (B) and (C). Reproduced from ref. 77 with permission from The Royal Society of Chemistry.

In 2011, Zhao's group synthesised a novel uniform core–shell nanostructure with LDH as the core and ordered mesoporous silica as the shell.[77] The morphology of this core–shell nanocomposite observed under TEM is interesting, showing two types of nanostructures (Fig. 9A): (1) mesoporous nanoplates, and (2) rod-like cores covered by ordered mesoporous silica.[77] These two nanostructures are suggested to be projections of LDH@SiO_2 nanocomposites from two perpendicular directions (Fig. 9A).[77] By adjusting the amount of TEOS, the average thickness of the mesoporous silica shell could be tuned between 20 and 50 nm.[77] The LDH@SiO_2 nanocomposites retain the properties of both LDH and SiO_2, including high drug loading capacity, dispersivity and biocompatibility, sustained release of anionic drugs, and ready surface modification.[77] Meanwhile, Liu *et al.* synthesised a LDH@SiO_2 nanostructure for drug delivery (Fig. 9B).[78] Although the particles were less controllable in morphology compared with Zhao group's work, they still showed sustained release of the drug and other important properties for drug delivery.[78]

Apart from being a drug carrier,[79,80] the LDH@SiO_2 nanocomposite has been investigated as a catalyst precursor.[81] Shi's group fabricated a multi-nanoparticle-embedded core@mesoporous silica shell structure.[81] The core consisted of aluminium/magnesium oxides (that were then converted to LDH) and Au nanoparticles, in which the aluminium/magnesium oxides provided an essential support for Au nanoparticles, and the mesoporous silica shell offered the diffusion channels for reactants and products, allowing efficient access of reactants to the catalytic nanoparticles inside.[81]

4.2 LDH@protein

Protein is an amphiphilic biopolymer, and its interactions with LDH nanoparticles provide a new way to stabilise the colloidal stability, and moreover, to deliver protein/peptide-based drugs. There are a few investigations on the interactions between LDH nanoparticles and various proteins. An *et al.*

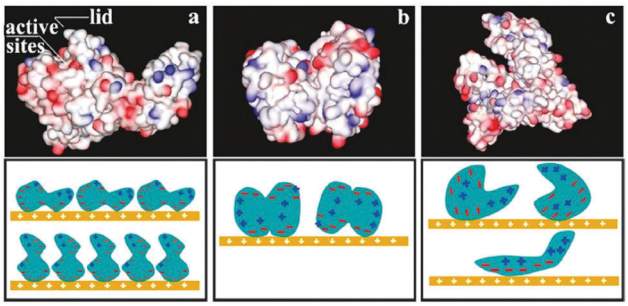

Fig. 10 Top images show electrostatic surface potentials for (a) porcine pancreatic lipase, (b) haemoglobin, (c) bovine serum albumin at pH 7.4. Bottom pictures schematically illustrate possible orientations of (a) porcine pancreatic lipase, (b) haemoglobin, (c) bovine serum albumin on the positively charged 2D LDH surface. Reproduced from ref. 82 with permission.

assembled protein-adsorbed LDH nanosheets in HCl-Tris buffer, and studied the conformations and orientations of three adsorbed proteins (porcine pancreatic lipase (PPL), haemoglobin (Hb), and bovine serum albumin (BSA)) (Fig. 10).[82] The structure and conformations of PPL were well retained because of negative charges concentrated on the side opposite to the active centres, and the orientations of PPL could be lying flat or standing up depending on the ratio of PPL and LDH (Fig. 10a). The bioactivity of PPL was thus enhanced in the hydrolysis and kinetic resolution in comparison with its soluble counterpart. The secondary structure and redox-active heme groups of Hb were not denatured either, but its tertiary or quaternary structure was changed through unfolding (Fig. 10b). The negative charges on the BSA surface were distributed along the linearly arranged domain I and II, resulting in the unfolded secondary structure (Fig. 10c). Therefore, the conformation and orientation of proteins on LDH nanosheets are dependent on the charge distribution and structural features of the proteins. These authors further suggested that the LDH nanosheet could improve the activity and stereoselectivity of at least some lipases.[82]

Kong *et al.* reported the assembled LDH nanosheets with Hb and horseradish peroxidase *via* the layer by layer deposition technique. They found that the assembled protein/LDH electrode showed remarkable electrocatalytic activity towards oxidation of catechol in a wide linear response range, a low detection limit, high stability and reproducibility.[83] Bellezza *et al.* observed that proteins (myoglobin and BSA) strongly interacted with NiAl–LDH or NiCr–LDH nanoparticles and exhibited a Langmuir-type adsorption.[84,85]

Our group also constructed the LDH nanocomposites with ovalbumin (OVA) (Fig. 11A) and BSA coating to modulate immune response and improve LDH stability, respectively.[86,87] The adsorption of OVA and BSA on LDH nanoparticles was well fitted with the Langmuir model (Fig. 11B and C); the maximum monolayer adsorption capacity was 0.58 mg mg^{-1} for OVA (Fig. 11B),[86] and 0.70 mg mg^{-1} for BSA (Fig. 11C) on 110 nm LDH nanoparticles.[87] Coating OVA on LDH demonstrated that LDH as an adjuvant induced a high level of IgG1 antibodies comparable to Alum (an FDA approved adjuvant for human vaccination) but with much weaker inflammation.[86] BSA pre-coating prevented LDH

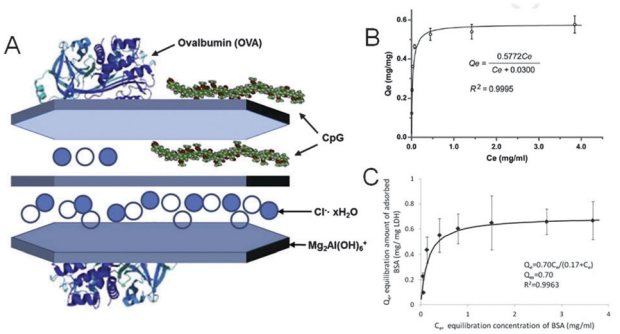

Fig. 11 (A) Schematic illustration of the Mg_2Al–LDH-based adjuvant–antigen hybrid system with OVA surface-adsorbed and CpG surface-adsorbed or intercalated. (B, C) OVA or BSA adsorption isotherm over Mg_2Al–LDH nanoparticles, and data are expressed as mean ± SD and mean ± SEM respectively. Reproduced from ref. 86 and 87 with permission.

and drug/gene-loaded LDH from aggregation in the electrolyte solution (physiological environment) and enhanced the cellular uptake, possibly due to the improved colloidal stability of nanoparticles in the culture medium solution.[87]

4.3 LDH@polymer

There are two main methods to functionalise LDH nanoparticles with polymers: (1) adsorption of pre-synthesised polymers *via* electrostatic interaction,[19,88–90] (2) *in situ* polymerisation, including one-pot *in situ* polymerisation,[91] surface-initiated atom transfer radical polymerisation (ATPR),[92,93] and crosslinking.[94] Adsorption of anionic polymers on the LDH surface can be achieved by simply mixing the two components or *via* electrodeposition. This synthesis method takes advantages of the positive charge on the LDH surface, thus the conjugated polymers are required to be negatively charged. Because of its facile procedure, adsorption is the most common method used to synthesise LDH@polymer nanocomposites. One-pot *in situ* polymerisation uses LDH nanoparticles as the template/core to polymerise the anionic monomers, without washing and transferring steps. In this method, the monomer is often anchored on the LDH core *via* electrostatic attraction. The surface-initiated ATPR originates from the atom transfer step, which allows uniform growth of the polymeric chains.[95] Moreover, the ATPR reaction can be achieved under environmentally friendly conditions using water as the solvent.[96] Cross-linking is usually achieved by covalently cross-linking polymers that are adsorbed on the LDH surface *via* a cross-linked agent (*e.g.* glutaraldehyde).[94]

The main application of LDH@polymer nanocomposites is drug/gene delivery. Hu *et al.* tailored the functionality of LDH surfaces through surface-initiated ATPR of 2-(dimethylamino)-ethyl methacrylates.[93] This LDH composite with the flexible polycation brushes (2-(dimethylamino)-ethyl methacrylates) demonstrated increased ability to condense plasmid DNA, and higher cellular uptake and gene transfection efficiency in COS7 and HepG2 cell lines.[93] Poly(ethylene glycol) (PEG) is considered a biocompatible polymer, and widely used to functionalise other drug delivery carriers with the aim of increasing

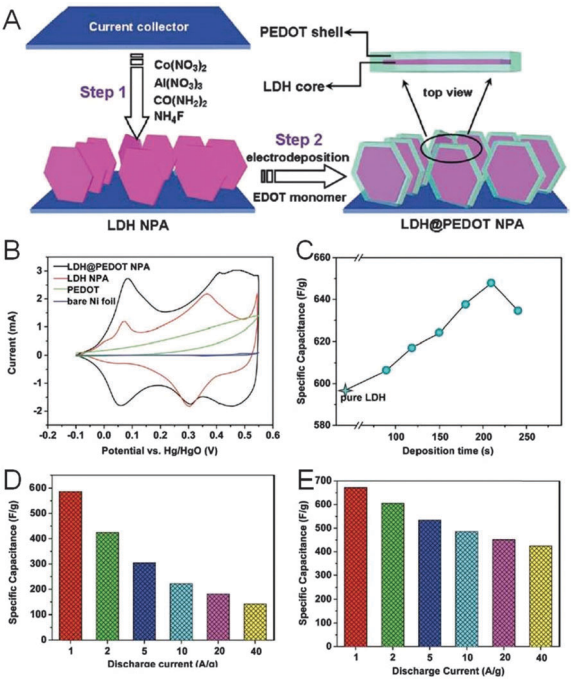

Fig. 12 (A) Schematic illustration of fabricating LDH@PEDOT core–shell nanoplatelet array (NPA) electrode. (B) Cyclic voltammetry curves of the LDH NPA, PEDOT, LDH@PEDOT NPA and bare Ni foil electrode measured at a scan rate of 2 mV s^{-1}. (C) Specific capacitance of the LDH@PEDOT NPA electrode as a function of deposition time. (D, E) Specific capacitance of pristine LDH NPA and LDH@PEDOT NPA electrodes, respectively, at various discharge current densities. Reproduced from ref. 19 with permission.

colloidal stability and circulation time.[97–99] For example, Li *et al.* synthesised anionic PEG functionalised LDH nanohybrids.[90] This LDH@PEG nanohybrid displayed enhanced colloidal stability and re-dispersing ability compared with LDH itself, due to the polymer steric hindrance and the electrostatic repulsion.[90] Colonic delivery is the other important area of LDH@polymer application. In order to improve the mucoadhesive ability and controlled release in acidic environments, the drug carrier LDH is coated with Eudragit or pectin to enhance the structural integrity in the acidic environment.[88,100–103]

The LDH@polymer is also applied for high-performance energy storage. Han *et al.* fabricated a LDH@poly(3,4-ethylenedioxythiophene) (PEDOT) core–shell nanoplatelet array (NPA) grown on a flexible Ni foil substrate as a high performance pseudocapacitor (Fig. 12A), in which the LDH core provided high energy storage capacity, and the polymer shell and its porous structure facilitated electron/mass transport in the redox reaction.[19] The LDH@PEDOT core–shell NPA showed a maximum specific capacitance of 649 F g^{-1} by cyclic voltammetry (scan rate was 2 mV s^{-1}) and 672 F g^{-1} by galvanostatic discharge (current density was 1 A g^{-1}) (Fig. 12B and C).[19] The specific capacitance of the well-arranged LDH@PEDOT NPA (672 F g^{-1}) was much higher than its counterpart LDH@PEDOT–Ni foam (334 F g^{-1}), indicating that the mesoporous and well-ordered structure enhances ion diffusion of the electrolyte and electron transfer.[19]

4.4 LDH@organic hydrophobic modifier

Different from polymers, the organic modifiers with much smaller molecular weight are anchored on the LDH surface with the aim of modifying LDH's intrinsic hydrophilic properties.

The organic modifiers include various surfactants (such as sodium dodecyl sulphate, dodecylsulfonate, and dodecylbenzenesulfonate) and other anionic organic molecules (hexanoic acid and silane coupling agents).[89,104–108] Hydrophobic modification of LDH is applied in drug delivery of hydrophobic pesticides and dyes,[106,107] as well as in biofuel production.[105,108] It is worth noting that some of the organic modifiers are not only anchored on the surface of the LDH matrix, but also intercalated in the LDH gallery space, and the ionic affinity of the molecules may allow partial exchange of anions between LDH layers.

5. Dot-coated LDH nanocomposites

Recently, dot-coated LDH nanocomposites as a group of new hierarchical hybrid materials have attracted interest. The dot-coated LDH consists of an LDH substrate and other smaller sphere-shaped nanodots coated on the surface of LDH (Fig. 1C). Different from the LDH@shell nanocomposites, the surface of LDH is only partly covered by coated dots, thus presenting a new hierarchical structure of LDH nanocomposites and exhibiting some exciting advantages, such as the possibility of multi-functionalising LDH. Moreover, the increased particle surface roughness could also enhance cell binding and subsequent engulfment by cells in biomedical applications.[109] The coating nanomaterials that have been developed include metal nanoparticles (*e.g.* Au nanoparticles, Pd nanoparticles, and Ag nanoparticles) and SiO_2 nanoparticles,[17,18,110,111] and the synthesised dot-coated LDHs have been examined in drug delivery and simultaneous bio-imaging, and catalysis.

5.1 Metal nanoparticle dot-coated LDH

Shi's group reported Gd-doped LDH@Au nanocomposites to dually function as a drug carrier and a diagnostic agent.[18] As claimed by the authors, the advantage of this nanocomposite over other nano-systems is that the imaging agents (*i.e.* Gd^{3+} and Au nanoparticles) can be easily and effectively introduced into LDH and thus form the unique dot-coated nanocomposite structure. In this structure, Gd^{3+} as the magnetic resonance imaging contrast agent was doped in the LDH lattice *via* the coprecipitation method, and Au nanoparticles with an average diameter of 3.4 nm were incorporated in the nanocomposite by depositing $Au(OH)_3$ on the surface of LDH under alkaline conditions, followed by the reduction with $NaBH_4$ (Fig. 13A and B).[18] This LDH–Gd@Au nanocomposite had an average hydrodynamic diameter of around 140 nm, and was well-dispersed in water (Fig. 13C).[18] By culturing mouse fibroblastic cell lines and human cervical cancer cell lines *in vitro*, the authors showed enhanced doxorubicin delivery efficiency with LDH–Gd@Au compared with free doxorubicin (Fig. 13D).[18] Meanwhile, thanks to the component of Gd^{3+} and Au, the LDH–Gd@Au nanocomposite acted efficiently as a dual-functional contrast agent for magnetic resonance imaging and X-ray computed tomography imaging in a tumour-bearing mice model (Fig. 13E).[18]

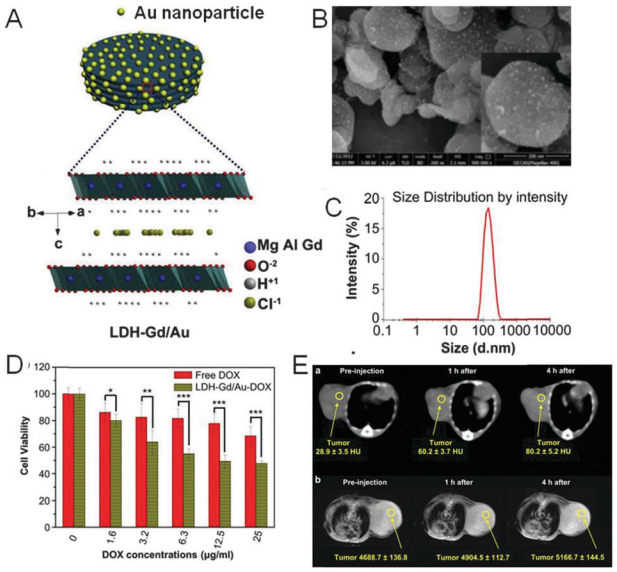

Fig. 13 (A) Schematic illustration, (B) SEM images, and (C) dynamic light scattering size distribution of LDH–Gd@Au nanocomposites. (D) HeLa cell viabilities when exposed to free doxorubicin and LDH–Gd@Au–doxorubicin at concentrations of 0–25 μg ml^{-1} (*$p < 0.05$, **$p < 0.01$, ***$p < 0.001$). (E) X-ray CT (upper images) and MRI (bottom images) imaging of tumour after intravenous injection of LDH–Gd@Au–heparin in 4T1 murine breast tumour-bearing mice for 0, 1, 4 h. Modified and reproduced from ref. 18 with permission.

Zhao *et al.* anchored finely dispersed Pd nanodots (~1.8 nm) to CoAl–LDH nanoparticles (~1.5 μm) *via* a facile *in situ* redox reaction between the Co^{2+} in LDH nanoparticles and the $PdCl_4^{2-}$ precursor.[17] This architecture showed enhanced catalytic activity and robust durability towards ethanol electro-oxidation compared with the commercial Pd/C catalyst, in which LDH played a ternary role: a catalyst support, a stabiliser of Pd nanodots, and a reducing agent (without any external agent).[17] Zhao *et al.* claimed that this work provided a promising approach to fabricating highly efficient nanocatalysts that could be used in fuel cells and other related catalytic reactions.[17]

Apart from these two examples in biomedical and catalytic applications, metal nanoparticles, such as Ag nanoparticles and quantum dots, have also been dot-coated onto the surface of LDH and investigated in the field of sterilisation and light emitting diodes.[110,112,113]

5.2 SiO_2 nanoparticle dot-coated LDH

Our group recently synthesised amine-functionalised SiO_2 dot-coated LDH (LDH@SiO_2–NH_2) nanocomposites *via* electrostatic interactions and condensation of APTES (Fig. 14a).[111] This synthesis strategy is different from the one for LDH@SiO_2 discussed in Section 4.1, with the purpose of fabricating the dot-coated nanostructure instead of the core–shell structure. SiO_2 nanodots (*Z*-average size of 10–15 nm, zeta potential of

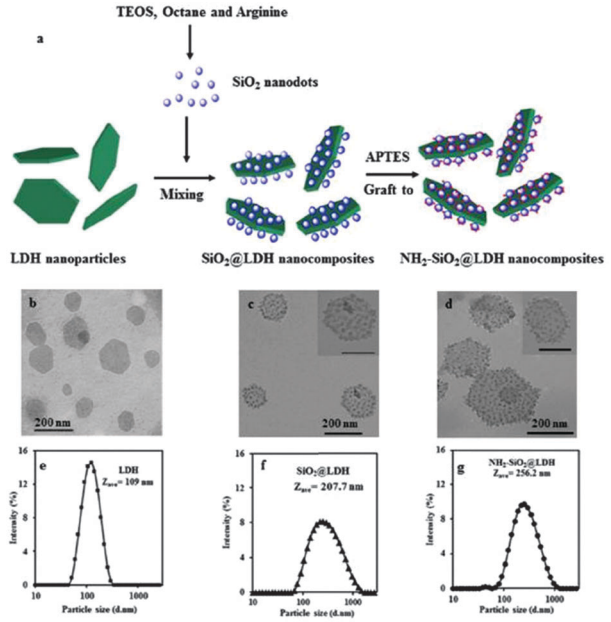

Fig. 14 (a) Schematic illustration of the synthetic process and proposed structures of functional LDH@SiO_2 nanocomposites. (b–d) TEM images of LDH (b), LDH@SiO_2 (c), and LDH@SiO_2–NH_2 (d), and the scale bars of the inset are 100 nm. (e–g) Particle size distribution of LDH (e), LDH@SiO_2 (f), and LDH@SiO_2–NH_2 (g). Reproduced from ref. 111 with permission.

−38.8 mV) and LDH nanoparticles (approximately 110 nm, +42.5 mV) were synthesised separately, and then mixed to form LDH@SiO_2 nanocomposites *via* electrostatic attraction.[111] The nanocomposites were modified with –NH_2 by condensing APTES on the surface.[111]

The resulted LDH@SiO_2–NH_2 had the average hydrodynamic diameter of 256 nm, and showed uniform SiO_2 nanodots of around 10–15 nm attached on the surface of LDH (Fig. 14b–g).[111] The amine-functionalised SiO_2 dot-coating improved LDH dispersion in the culture medium and PBS, and more importantly enhanced siRNA delivery to the U2OS cell line to inhibit cell proliferation, probably due to the improved nanoparticle dispersion.[111] We also suggest that the enhanced endosomal escape increases cell death,[111] in comparison with the positively charged silica nanoparticles,[114] which seems to be less capable for the proton sponge effect.

6. LDH@targeting moiety

There are numerous barriers for nanoparticle-based drug carriers en route to their target, such as mucosal barriers and non-specific uptake.[115–117] Thus it is necessary to combine the rational design of nanocarriers with moieties to encourage active targeting. This may also allow a more favourable benefit-risk profile by reducing organ toxicity, which often limits the clinical effectiveness of anthracyclines. Indeed, as tumour-free survival improves with novel chemotherapeutics, their impact of overall survival is often limited by organ toxicity, which could be potentially mitigated by nanocomposite-based drug delivery.[118] In the case of LDH nanocarriers, recent progress in targeting moiety design has been seen in conjugating folic acid and antibody agents.[20,57,119–121]

Folic acid has a high affinity ($K_d \approx 100$ pM) for folate receptors which are often overexpressed in various human cancers, such as ovary, lung, kidney, colon cancer, *etc.*[122–125] By conjugating this cancer cell specific ligand on LDHs, Choy's group described the selectivity of this nanohybrid to folate receptor-overexpressed cell lines (*i.e.* human nasopharyngeal epidermoid carcinoma cells) in comparison with folate receptor deficient cell lines (*i.e.* human lung adenocarcinoma epithelial cells).[20] It is worth noting that the anionic type of folic acid can be intercalated into the LDH gallery space, which may result in the targeting function of folic acid being shielded.[126–128] To address this issue, the researchers from the same group grafted folic acid on the surface of LDH by covalent coupling using silane coupling reagents APTES and 1-ethyl-3-(3-dimethylaminopropyl)-carbodiimide (EDC).[20] To do this, the surface of LDH nanoparticles was modified with APTES, whose amine end group could be conjugated with the functional groups such as carboxylate and thiocyanate.[20] For example, the activated carboxyl group of folic acid by *N*-hydroxysuccinimide, using EDC as a coupling agent, was then combined with the amine end group of APTES on the surface of LDH to form LDH@folic acid composites.[20]

To target vascular injury caused by surgical treatment (*e.g.* angioplasty), our group conjugated anti-coagulant drug low molecular weight heparin (LMWH)-intercalated LDH nanoparticles with a cross-linked fibrin antibody (an antibody that rapidly accumulates at the site of vascular injury and remains for many weeks) by associating the sulfhydryl-modified antibody with the maleimide-containing LMWH.[121,129–131] With this LMWH–LDH@antibody, we observed specific delivery of drugs to the site of injury, reduced luminal loss and thrombotic occlusion in a rat model of arterial injury.[121]

7. Conclusions and perspective

This feature article summarises the recent progress in synthesis approaches, physicochemical properties, and potential applications of LDH-based nanocomposites. The hierarchical LDH nanocomposites, combining the advantages of LDH nanoparticles/nanosheets and other nanomaterials/molecules, do not only show the advantages over each component of the nanocomposites, but also show some superiority to other nanomaterials such as polymers, metal oxide and mesoporous silica nanoparticles, when they are applied in drug delivery, imaging, water purification, catalysis, and energy storage. Some exciting research contributions are highlighted in this feature article to illustrate the unique structures, excellent properties, and important applications of the hierarchical LDH nanocomposites. In particular, the synthesis and application of dot-coated LDH nanocomposites is a new and emerging area, and worthy of further investigation, due to the virus-like surface of dot-coated LDH nanocomposites and the availability for multi-functionalisation.

Although there have been rapid advances in the synthesis and application studies of LDH-based nanocomposites, it is still a newly emerging area and there is a great deal of room for researchers to explore in this area. Constructing a new hierarchical structure will not only provide a new conceptual structure and synthesis approach, but will also offer an opportunity for potential applications. When an LDH-based nanocomposite is designed and synthesised, it is a priority question to consider whether the nanocomposite takes full use of LDH and other nanomaterials. By fabricating LDHs with different metal cations and anions, LDH could be a candidate to be used for different modes of bio-imaging as contrast agents, production of a number of compounds as catalysts, and delivery of various therapeutic molecules.

Towards the final goal of transferring LDH-based nanocomposites from bench to industry, there are several challenges to address. One of the major challenges is to simplify the synthesis process with precise control of particle size and morphology. This is also the prerequisite for scale-up. For LDH-based nanocomposites to be used in clinics, the colloidal stability of the nanocomposites also needs to be considered, as the aggregated particles would lower the therapeutic efficacy or even block the blood vessel to cause the clot eventually. The lack of bio-safety and the bio-distribution profile for healthcare application is another challenge. Future research should focus on closely linking up the nanocomposite physicochemical properties with practical applications, including, but not limited to, therapeutics, diagnosis, water and air purification, energy storage, and energy conversion.

Acknowledgements

This work was financially supported by National Health and Medical Research Council of Australia (NHMRC) Early Career Fellowship APP1073591, and Australian Research Council (ARC) Future Fellowship FT120100813.

Notes and references

1 A. Burns, H. Ow and U. Wiesner, *Chem. Soc. Rev.*, 2006, **35**, 1028–1042.
2 R. G. Chaudhuri and S. Paria, *Chem. Rev.*, 2012, **112**, 2373–2433.
3 G. D. Li and Z. Y. Tang, *Nanoscale*, 2014, **6**, 3995–4011.
4 N. V. Long, Y. Yang, C. M. Thi, N. V. Minh, Y. Q. Cao and M. Nogami, *Nano Energy*, 2013, **2**, 636–676.
5 C. Y. Li, C. Ma, F. Wang, Z. J. Xi, Z. F. Wang, Y. Deng and N. Y. He, *J. Nanosci. Nanotechnol.*, 2012, **12**, 2964–2972.
6 S. Y. Wei, Q. Wang, J. H. Zhu, L. Y. Sun, H. F. Lin and Z. H. Guo, *Nanoscale*, 2011, **3**, 4474–4502.
7 Y. Chen, H. R. Chen, D. P. Zeng, Y. B. Tian, F. Chen, J. W. Feng and J. L. Shi, *ACS Nano*, 2010, **4**, 6001–6013.
8 P. S. Braterman, Z. P. Xu and F. Yarberry, Layered double hydroxides (LDHs), in *Handbook of Layered Materials*, ed. S. M. Auerbach, K. A. Carrado and P. K. Dutta, Marcel Dekker, New York, 2004, ch. 8, pp. 373–474.
9 Z. P. Xu, G. S. Stevenson, C. Q. Lu, G. Q. M. Lu, P. F. Bartlett and P. P. Gray, *J. Am. Chem. Soc.*, 2006, **128**, 36–37.
10 E. Gardner, K. M. Huntoon and T. J. Pinnavaia, *Adv. Mater.*, 2001, **13**, 1263–1266.
11 Y. Arai and M. Ogawa, *Appl. Clay Sci.*, 2009, **42**, 601–604.
12 Q. Wang and D. O'Hare, *Chem. Rev.*, 2012, **112**, 4124–4155.
13 J. Liu, S. Z. Qiao, J. S. Chen, X. W. Lou, X. R. Xing and G. Q. Lu, *Chem. Commun.*, 2011, **47**, 12578–12591.
14 H. Zhang, D. K. Pan, K. Zou, J. He and X. Duan, *J. Mater. Chem.*, 2009, **19**, 3069–3077.
15 C. P. Chen, P. H. Wang, T. T. Lim, L. H. Liu, S. M. Liu and R. Xu, *J. Mater. Chem. A*, 2013, **1**, 3877–3880.
16 Q. Chang, L. H. Zhu, Z. H. Luo, M. Lei, S. C. Zhang and H. Q. Tang, *Ultrason. Sonochem.*, 2011, **18**, 553–561.
17 J. W. Zhao, M. F. Shao, D. P. Yan, S. T. Zhang, Z. Z. Lu, Z. X. Li, X. Z. Cao, B. Y. Wang, M. Wei, D. G. Evans and X. Duan, *J. Mater. Chem. A*, 2013, **1**, 5840–5846.
18 L. J. Wang, H. Y. Xing, S. J. Zhang, Q. G. Ren, L. M. Pan, K. Zhang, W. B. Bu, X. P. Zheng, L. P. Zhou, W. J. Peng, Y. Q. Hua and J. L. Shi, *Biomaterials*, 2013, **34**, 3390–3401.
19 J. B. Han, Y. B. Dou, J. W. Zhao, M. Wei, D. G. Evans and X. Duan, *Small*, 2013, **9**, 98–106.
20 J. M. Oh, S. J. Choi, G. E. Lee, S. H. Han and J. H. Choy, *Adv. Funct. Mater.*, 2009, **19**, 1617–1624.
21 L. O. Torres-Dorante, J. Lammel, H. Kuhlmann, T. Witzke and H. W. Olfs, *J. Plant Nutr. Soil Sci.*, 2008, **171**, 777–784.
22 Z. P. Xu, Q. H. Zeng, G. Q. Lu and A. B. Yu, *Chem. Eng. Sci.*, 2006, **61**, 1027–1040.
23 C. Mousty, *Appl. Clay Sci.*, 2004, **27**, 159–177.
24 K. H. Goh, T. T. Lim and Z. Dong, *Water Res.*, 2008, **42**, 1343–1368.
25 B. F. Sels, D. E. De Vos and P. A. Jacobs, *Catal. Rev.: Sci. Eng.*, 2001, **43**, 443–488.
26 T. Stimpfling and F. Leroux, *Chem. Mater.*, 2010, **22**, 974–987.
27 Z. Gu, A. C. Thomas, Z. P. Xu, J. H. Campbell and G. Q. Lu, *Chem. Mater.*, 2008, **20**, 3715–3722.
28 Z. Gu, A. Wu, L. Li and Z. P. Xu, *Pharmaceutics*, 2014, **6**, 235–248.
29 Y. F. Xu, Y. C. Dai, J. Z. Zhou, Z. P. Xu, G. R. Qian and G. Q. M. Lu, *J. Mater. Chem.*, 2010, **20**, 4684–4691.
30 Z. Y. Lu, W. Zhu, X. D. Lei, G. R. Williams, D. O'Hare, Z. Chang, X. M. Sun and X. Duan, *Nanoscale*, 2012, **4**, 3640–3643.
31 M. Adachi-Pagano, C. Forano and J. P. Besse, *Chem. Commun.*, 2000, 91–92.
32 S. O'Leary, D. O'Hare and G. Seeley, *Chem. Commun.*, 2002, 1506–1507.
33 T. Hibino and W. Jones, *J. Mater. Chem.*, 2001, **11**, 1321–1323.
34 G. Hu, N. Wang, D. O'Hare and J. J. Davis, *J. Mater. Chem.*, 2007, **17**, 2257–2266.
35 G. Hu, N. Wang, D. O'Hare and J. Davis, *Chem. Commun.*, 2006, 287–289.
36 W. R. Zhao, J. L. Gu, L. X. Zhang, H. R. Chen and J. L. Shi, *J. Am. Chem. Soc.*, 2005, **127**, 8916–8917.
37 F. Wypych, G. A. Bubniak, M. Halma and S. Nakagaki, *J. Colloid Interface Sci.*, 2003, **264**, 203–207.
38 Y. Wang, W. S. Yang and J. J. Yang, *Electrochem. Solid-State Lett.*, 2007, **10**, A233–A236.
39 H. Zhang, D. K. Pan and X. Duan, *J. Phys. Chem. C*, 2009, **113**, 12140–12148.
40 H. Zhang, K. Zou, H. Sun and X. Duan, *J. Solid State Chem.*, 2005, **178**, 3485–3493.
41 C. P. Chen, L. K. Yee, H. Gong, Y. Zhang and R. Xu, *Nanoscale*, 2013, **5**, 4314–4320.
42 D. K. Pan, H. Zhang, T. Fan, J. G. Chen and X. Duan, *Chem. Commun.*, 2011, **47**, 908–910.
43 Y. Zhao, S. He, M. Wei, D. G. Evans and X. Duan, *Chem. Commun.*, 2010, **46**, 3031–3033.
44 M. F. Shao, F. Y. Ning, Y. F. Zhao, J. W. Zhao, M. Wei, D. G. Evans and X. Duan, *Chem. Mater.*, 2012, **24**, 1192–1197.
45 M. F. Shao, F. Y. Ning, J. W. Zhao, M. Wei, D. G. Evans and X. Duan, *J. Am. Chem. Soc.*, 2012, **134**, 1071–1077.
46 J. Wang, R. R. Zhu, B. Gao, B. Wu, K. Li, X. Y. Sun, H. Liu and S. L. Wang, *Biomaterials*, 2014, **35**, 466–478.
47 X. F. Zhang, J. Wang, R. M. Li, Q. H. Dai, R. Gao, Q. Liu and M. L. Zhang, *Ind. Eng. Chem. Res.*, 2013, **52**, 10152–10159.
48 A. N. Ay, D. Konuk and B. Zumreoglu-Karan, *Mater. Sci. Eng., C*, 2011, **31**, 851–857.
49 D. A. Li, Y. T. Zhang, M. Yu, J. Guo, D. Chaudhary and C. C. Wang, *Biomaterials*, 2013, **34**, 7913–7922.
50 D. H. Park, J. E. Kim, J. M. Oh, Y. G. Shul and J. H. Choy, *J. Am. Chem. Soc.*, 2010, **132**, 16735–16736.
51 L. Li, R. Z. Ma, N. Iyi, Y. Ebina, K. Takada and T. Sasaki, *Chem. Commun.*, 2006, 3125–3127.

52 R. Z. Ma and T. Sasaki, *Adv. Mater.*, 2010, **22**, 5082–5104.
53 L. Li, Y. J. Feng, Y. S. Li, W. R. Zhao and J. L. Shi, *Angew. Chem., Int. Ed.*, 2009, **48**, 5888–5892.
54 L. Huang, D. C. Chen, Y. Ding, S. Feng, Z. L. Wang and M. L. Liu, *Nano Lett.*, 2013, **13**, 3135–3139.
55 X. T. Chen, F. Mi, H. Zhang and H. Q. Zhang, *Mater. Lett.*, 2012, **69**, 48–51.
56 H. Zhang, R. Qi, D. G. Evans and X. Duan, *J. Solid State Chem.*, 2004, **177**, 772–780.
57 Z. Gu, B. E. Rolfe, A. C. Thomas and Z. P. Xu, *Curr. Pharm. Des.*, 2013, **19**, 6330–6339.
58 A. N. Ay, B. Zumreoglu-Karan, A. Temel and V. Rives, *Inorg. Chem.*, 2009, **48**, 8871–8877.
59 S. Mornet, S. Vasseur, F. Grasset and E. Duguet, *J. Mater. Chem.*, 2004, **14**, 2161–2175.
60 A. K. Gupta and M. Gupta, *Biomaterials*, 2005, **26**, 3995–4021.
61 K. Shang, J. Y. Zhu, X. M. Meng, Z. Q. Cheng and S. Y. Ai, *Biosens. Bioelectron.*, 2012, **37**, 107–111.
62 S. K. Khetan and T. J. Collins, *Chem. Rev.*, 2007, **107**, 2319–2364.
63 D. K. Pan and H. Zhang, *Acta Chim. Sin.*, 2011, **69**, 1545–1552.
64 C. M. Dai, S. U. Geissen, Y. L. Zhang, Y. J. Zhang and X. F. Zhou, *Environ. Pollut.*, 2011, **159**, 1660–1666.
65 Z. P. Xu, R. Xu and H. C. Zeng, *Nano Lett.*, 2001, **1**, 703–706.
66 Z. Hasan, J. Jeon and S. H. Jhung, *J. Hazard. Mater.*, 2012, **209**, 151–157.
67 X. M. Liu, Z. D. Huang, S. W. Oh, B. Zhang, P. C. Ma, M. M. F. Yuen and J. K. Kim, *Compos. Sci. Technol.*, 2012, **72**, 121–144.
68 H. Li, Z. X. Wang, L. Q. Chen and X. J. Huang, *Adv. Mater.*, 2009, **21**, 4593–4607.
69 M. C. Orilall and U. Wiesner, *Chem. Soc. Rev.*, 2011, **40**, 520–535.
70 N. T. H. Trang, H. V. Ngoc, N. Lingappan and D. J. Kang, *Nanoscale*, 2014, **6**, 2434–2439.
71 B. Wang, G. R. Williams, Z. Chang, M. Jiang, J. Liu, X. Lei and X. Sun, *ACS Appl. Mater. Interfaces*, 2014, **6**, 16304–16311.
72 Y. H. Gu, Z. Y. Lu, Z. Chang, J. F. Liu, X. D. Lei, Y. P. Li and X. M. Sun, *J. Mater. Chem. A*, 2013, **1**, 10655–10661.
73 Z. Y. Lu, Z. Chang, W. Zhu and X. M. Sun, *Chem. Commun.*, 2011, **47**, 9651–9653.
74 W. Zhu, Z. Y. Lu, G. X. Zhang, X. D. Lei, Z. Chang, J. F. Liu and X. M. Sun, *J. Mater. Chem. A*, 2013, **1**, 8327–8331.
75 Z. Tang, C. H. Tang and H. Gong, *Adv. Funct. Mater.*, 2012, **22**, 1272–1278.
76 C. Guan, X. L. Li, Z. L. Wang, X. H. Cao, C. Soci, H. Zhang and H. J. Fan, *Adv. Mater.*, 2012, **24**, 4186–4190.
77 H. F. Bao, J. P. Yang, Y. Huang, Z. P. Xu, N. Hao, Z. X. Wu, G. Q. Lu and D. Y. Zhao, *Nanoscale*, 2011, **3**, 4069–4073.
78 J. Liu, R. Harrison, J. Z. Zhou, T. T. Liu, C. Z. Yu, G. Q. Lu, S. Z. Qiao and Z. P. Xu, *J. Mater. Chem.*, 2011, **21**, 10641–10644.
79 J. H. Yang, S. Y. Lee, Y. S. Han, K. C. Park and J. H. Choy, *Bull. Korean Chem. Soc.*, 2003, **24**, 499–503.
80 S. H. Hwang, S. C. Jung, S. M. Yoon and D. K. Kim, *J. Phys. Chem. Solids*, 2008, **69**, 1061–1065.
81 L. J. Wang, J. L. Shi, Y. Zhu, Q. J. He, H. Y. Xing, J. Zhou, F. Chen and Y. Chen, *Langmuir*, 2012, **28**, 4920–4925.
82 Z. An, S. Lu, J. He and Y. Wang, *Langmuir*, 2009, **25**, 10704–10710.
83 X. G. Kong, X. Y. Rao, J. B. Han, M. Wei and X. Duan, *Biosens. Bioelectron.*, 2010, **26**, 549–554.
84 F. Bellezza, A. Alberani, T. Posati, L. Tarpani, L. Latterini and A. Cipiciani, *J. Inorg. Biochem.*, 2012, **106**, 134–142.
85 F. Bellezza, A. Cipiciani, L. Latterini, T. Posati and P. Sassi, *Langmuir*, 2009, **25**, 10918–10924.
86 S. Yan, B. E. Rolfe, B. Zhang, Y. H. Mohammed, W. Gu and Z. P. Xu, *Biomaterials*, 2014, **35**, 9508–9516.
87 Z. Gu, H. Zuo, A. Wu and Z. P. Xu, 3rd Symposium on Innovative Polymers for Controlled Delivery, Suzhou, China, 2014, accepted.
88 B. X. Li, J. He, D. G. Evans and X. Duan, *Int. J. Pharm.*, 2004, **287**, 89–95.
89 J. U. Ha and M. Xanthos, *Appl. Clay Sci.*, 2010, **47**, 303–310.
90 D. X. Li, X. J. Xu, J. Xu and W. G. Hou, *Colloids Surf., A*, 2011, **384**, 585–591.
91 X. J. Guo, L. H. Zhao, L. Zhang and J. Li, *Appl. Surf. Sci.*, 2012, **258**, 2404–2409.
92 H. Hu, X. B. Wang, S. L. Xu, W. T. Yang, F. J. Xu, J. Shen and C. Mao, *J. Mater. Chem.*, 2012, **22**, 15362–15369.
93 H. Hu, K. M. Xiu, S. L. Xu, W. T. Yang and F. J. Xu, *Bioconjugate Chem.*, 2013, **24**, 968–978.
94 P. R. Wei, S. H. Cheng, W. N. Liao, K. C. Kao, C. F. Weng and C. H. Lee, *J. Mater. Chem.*, 2012, **22**, 5503–5513.
95 K. Matyjaszewski and J. H. Xia, *Chem. Rev.*, 2001, **101**, 2921–2990.
96 N. Singh, J. Wang, M. Ulbricht, S. R. Wickramasinghe and S. M. Husson, *J. Membr. Sci.*, 2008, **309**, 64–72.
97 L. E. van Vlerken, T. K. Vyas and M. M. Amiji, *Pharm. Res.*, 2007, **24**, 1405–1414.
98 D. E. Owens and N. A. Peppas, *Int. J. Pharm.*, 2006, **307**, 93–102.
99 H. Otsuka, Y. Nagasaki and K. Kataoka, *Adv. Drug Delivery Rev.*, 2003, **55**, 403–419.
100 L. N. M. Ribeiro, A. C. S. Alcantara, M. Darder, P. Aranda, F. M. Araujo-Moreira and E. Ruiz-Hitzky, *Int. J. Pharm.*, 2014, **463**, 1–9.
101 V. Ambrogi, L. Perioli, M. Ricci, L. Pulcini, M. Nocchetti, S. Giovagnoli and C. Rossi, *Microporous Mesoporous Mater.*, 2008, **115**, 405–415.
102 M. del Arco, A. Fernandez, C. Martin and V. Rives, *J. Solid State Chem.*, 2010, **183**, 3002–3009.
103 V. Rives, M. del Arco and C. Martin, *J. Controlled Release*, 2013, **169**, 28–39.
104 B. Wang, H. Zhang, D. G. Evans and X. Duan, *Mater. Chem. Phys.*, 2005, **92**, 190–196.
105 M. R. Islam, Z. H. Guo, D. Rutman and T. J. Benson, *RSC Adv.*, 2013, **3**, 24247–24255.
106 J. F. Lu, K. Minami, S. Takami and T. Adschiri, *Chem. Eng. Sci.*, 2013, **85**, 50–54.
107 D. P. Qiu, Y. H. Li, X. Y. Fu, Z. Jiang, X. Y. Zhao, T. Wang and W. G. Hou, *Chin. J. Chem.*, 2009, **27**, 445–451.
108 J. Q. Jiang, Y. W. Zhang, Y. H. Zheng and P. K. Jiang, *Chem. Eng. Technol.*, 2013, **36**, 1371–1377.
109 A. E. Nel, L. Madler, D. Velegol, T. Xia, E. M. V. Hoek, P. Somasundaran, F. Klaessig, V. Castranova and M. Thompson, *Nat. Mater.*, 2009, **8**, 543–557.
110 J. C. Sun, J. J. Li, H. Fan and S. Y. Ai, *J. Mater. Chem. B*, 2013, **1**, 5436–5442.
111 L. Li, W. Gu, J. Liu, S. Yan and Z. P. Xu, *Nano Res.*, 2014, DOI: 10.1007/s12274-014-0552-6.
112 S. Cho, S. C. Hong and S. Kim, *J. Mater. Chem. C*, 2014, **2**, 450–457.
113 S. Cho, S. Jung, S. Jeong, J. Bang, J. Park, Y. Park and S. Kim, *Langmuir*, 2013, **29**, 441–447.
114 J. L. Vivero-Escoto, I. I. Slowing, B. G. Trewyn and V. S. Y. Lin, *Small*, 2010, **6**, 1952–1967.
115 M. J. Alonso, *Biomed. Pharmacother.*, 2004, **58**, 168–172.
116 P. Couvreur and C. Vauthier, *Pharm. Res.*, 2006, **23**, 1417–1450.
117 D. Peer, J. M. Karp, S. Hong, O. C. FaroKhzad, R. Margalit and R. Langer, *Nat. Nanotechnol.*, 2007, **2**, 751–760.
118 E. O. Hanrahan, A. M. Gonzalez-Angulo, S. H. Giordano, R. Rouzier, K. R. Broglio, G. N. Hortobagyi and V. Valero, *J. Clin. Oncol.*, 2007, **25**, 4952–4960.
119 Z. Y. Xia, N. Du, J. Q. Liu and W. G. Hou, *Chem. J. Chin. Univ.*, 2013, **34**, 596–600.
120 L. Yan, W. Chen, X. Y. Zhu, L. B. Huang, Z. G. Wang, G. Y. Zhu, V. A. L. Roy, K. N. Yu and X. F. Chen, *Chem. Commun.*, 2013, **49**, 10938–10940.
121 Z. Gu, B. E. Rolfe, Z. P. Xu, J. H. Campbell, G. Q. Lu and A. C. Thomas, *Adv. Healthcare Mater.*, 2012, **1**, 669–673.
122 D. J. Bharali, D. W. Lucey, H. Jayakumar, H. E. Pudavar and P. N. Prasad, *J. Am. Chem. Soc.*, 2005, **127**, 11364–11371.
123 C. P. Leamon and P. S. Low, *Drug Discovery Today*, 2001, **6**, 44–51.
124 P. S. Low, W. A. Henne and D. D. Doorneweerd, *Acc. Chem. Res.*, 2008, **41**, 120–129.
125 J. A. Reddy, V. M. Allagadda and C. P. Leamon, *Curr. Pharm. Biotechnol.*, 2005, **6**, 131–150.
126 A. M. Bashi, S. M. Haddawi and M. A. Mezaal, *Arabian J. Sci. Eng.*, 2013, **38**, 1663–1680.
127 J. H. Choy, J. S. Jung, J. M. Oh, M. Park, J. Jeong, Y. K. Kang and O. J. Han, *Biomaterials*, 2004, **25**, 3059–3064.
128 L. L. Qin, S. L. Wang, R. Zhang, R. R. Zhu, X. Y. Sun and S. D. Yao, *J. Phys. Chem. Solids*, 2008, **69**, 2779–2784.
129 A. C. Thomas and J. H. Campbell, *Thromb. Res.*, 2003, **109**, 65–69.
130 A. C. Thomas and J. H. Campbell, *Atherosclerosis*, 2004, **176**, 73–81.
131 A. C. Thomas and J. H. Campbell, *J. Controlled Release*, 2004, **100**, 357–377.

